MEASUREMENT OF ROTATIONAL MOTION IN MEMBRANES USING FLUORESCENCE RECOVERY AFTER PHOTOBLEACHING

LLOYD M. SMITH, ROBERT M. WEIS, AND HARDEN M. MCCONNELL, *Stauffer Laboratory for Physical Chemistry, Stanford University, Stanford, California 94305*

ABSTRACT A method has been developed for the measurement of the rotational motion of membrane components. In this method fluorescent molecules whose transition dipole moments lie in a given direction are preferentially destroyed with a short intense burst of polarized laser radiation. The fluorescence intensity, excited with a low intensity observation beam of polarized laser radiation, changes with time as the remaining fluorescent molecules rotate. The feasibility of the method has been demonstrated in a study of the rotation of the fluorescent lipid probe, diI ([bis-2-(*N*-octadecyl-3,3-dimethyl-l-benzo[*b*]pyrrole]-trimethincyanine iodide) incorporated into membranes composed of distearoylphosphatidylcholine (DSPC) or dipalmitoylphosphatidylcholine (DPPC) and 0–20 mol % cholesterol, below the main chain-melting transition temperatures of the phosphatidylcholines. Rotation times in the 0.6–800 s range were observed. The fluorescence recovery (or decay) curves are in satisfactory agreement with theoretical calculations.

INTRODUCTION

A significant problem in molecular and cell biology is the elucidation of the structures, functions, and composition of the cell surface. There is little doubt that the protein and lipid components of the plasma membrane play crucial roles in functions such as cell-surface recognition, triggering, and motility. It is likely that protein:protein and protein:lipid interactions are intimately involved in these processes. Information on these interactions has been obtained using fluorescence microscopy combined with photobleaching-recovery methods for the measurement of lateral motion in membranes (Smith and McConnell, 1978; Eldridge et al., 1980; Schlessinger et al., 1978; Sheetz et al., 1980). The measurement of the rotational motion of membrane components provides important additional information.

One technique currently used for measuring rotational motion of molecules in solutions is fluorescence anisotropy decay (Weber, 1973). This technique is limited in time scale by the fluorescence lifetime of the probe molecule (10–100 ns) and is therefore not suitable for the measurement of the rotational motion of membrane proteins. Spin-label paramagnetic resonance techniques can be used to measure longer rotational correlation times, up to a millisecond, but do not have high absolute sensitivity (number of detectable molecules) (Thomas, 1978; Hyde and Dalton, 1979; Gaffney, 1979; Rousselet et al., 1979).

Absorption (Nigg and Cherry, 1979; Cherry, 1978, 1979) or emission (Lo et al., 1980; Austin et al., 1979) measurements from long-lived triplet states extend the measurable

rotational times to milliseconds. However, longer rotational times are not accessible to these techniques.

In early measurements Cone (1972) and Brown (1972) utilized the intrinsic chromophore of rhodopsin to measure rotational times by observing the transient dichroism induced by photobleaching with polarized light. This method is limited to measurement on rhodopsin and other proteins containing intrinsic or attached extrinsic chromophores (e.g., Vaz et al., 1979). This method also lacks high absolute sensitivity. We report here the development and application of a conceptually similar but more sensitive fluorescence method for the measurement of rotational motion of protein and lipid components of membranes.

In this technique rotational motion is measured by first using a brief burst of intense polarized laser radiation to achieve orientational photoselection of fluorescent molecules. Fluorescent molecules having certain orientations are preferentially bleached and rendered nonfluorescent. The fluorescence intensity that results from the remaining fluorescent molecules is monitored using a polarized observation beam; this intensity changes with time as the molecules rotate. This method has been used to measure the rotation times of the fluorescent lipid probe [bis-2-(*N*-octadecyl-3,3-dimethyl-1-benzo [*b*]pyrrole)]-trimethincyanine iodide (diI)[1] in multibilayer membranes and in liposomes composed of distearoylphosphatidylcholine (DSPC) or dipalmitoylphosphatidylcholine (DPPC) and cholesterol at temperatures below the main chain-melting transition temperatures (θ_m) for the phospholipid. In these solid-phase membranes the measured rotational correlation times are remarkably large (up to minutes) and exhibit a strong temperature dependence.

EXPERIMENTAL

Cholesterol was recrystallized twice from ethanol and stored refrigerated under argon. DSPC and DPPC were obtained from Sigma Chemical Co. (St. Louis, Mo.) and used without further purification. The fluorescent lipid analogue diI was the generous gift of Dr. Alan Waggoner (Dept. of Chemistry, Amherst College, Amherst, Mass.) and was found to be pure by thin layer chromatography. Its structure is shown in Fig. 1.

Liposomes

Liposomes of DSPC (or DPPC) and cholesterol containing 0.005 mol % diI were prepared as follows. Appropriate amounts of lipid stock solutions in methanol or ethanol to give 1–2 μmol total lipid were combined in a 5-ml round-bottom flask and rotoevaporated to dryness. Chloroform ~0.5 ml) was added and the solution was rotoevaporated to a thin dry film. 1 ml of phosphate-buffered saline was added and the flask was stoppered and kept at a temperature above the main chain-melting phase transition (θ_m = 41°C for DPPC, 55°C for DSPC, Shimshick and McConnell, 1973) of the phosphatidylcholine for 15 min. The warm solution was vortexed for 2 s to give a liposomal suspension. For photobleaching measurements, 10 μl of the liposomal suspension were deposited in a ring of vacuum grease on a glass slide, and a cover slip pressed onto the top. Occasionally quartz slides and cover slips were used to reduce phosphorescence excited by the bleaching burst of radiation.

---

[1] *Abbreviations used in this paper:* DSPC, distearoylphosphatidylcholine; DDPC, dipalmitoylphosphatidylcholine; diI, [bis-2-(*N*-octadecyl-3,3-dimethyl-1-benzo[*b*]pyrrole)]trimethincyanine iodide; θ_m, the chain-melting transition temperatures of phosphatidylcholine; mol %, moles per 100 moles.

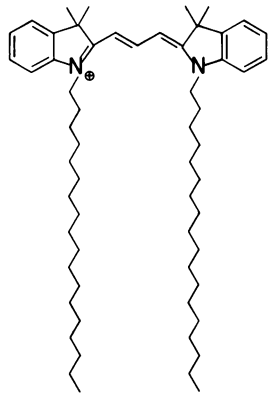

FIGURE 1 The fluorescent lipid probe diI.

Multibilayer Membranes

Multibilayer membranes were prepared as described by Rubenstein et al. (1979). Briefly, mixtures of the lipids in chloroform were prepared as described above for liposomes. The lipid solution was applied in drops to glass slides over an area smaller than the size of the cover slip (~0.5–1 μmol lipid per slide) at a temperature above θ_m of the phosphatidylcholine. The slides were hydrated in a chamber containing a water-saturated atmosphere at a temperature above θ_m for 24 h. Cover slips were then pressed on at a temperature above θ_m. These slides were returned to the chamber for 24–48 h until well-oriented as determined by microscopic examination under crossed polarizers.

Rotation Measurements

Two different experimental configurations were used in measurements of rotational motion. In the initial experiments bleaching was done using a Chromatix CMX-4 pulsed dye laser (Chromatix, Sunnyvale, Calif.) with the beam focused down to an ~20 μm Diam. Typically this gave a 50% bleach in a microsecond pulse. The laser dye used was Coumarin 522 (Exciton Chemical Co., Dayton, Ohio) at 533 nm with a power of ~2 mJ/pulse. A phototube (RCA C7164R; RCA ElectroOptics & Devices, RCA Solid State Div., Lancaster, Pa.) was protected from exposure to excess light during the bleach pulse using a gating circuit (GB1001A, EMI Gencom, Inc., Plainview, Penn.) to reverse temporarily the voltage on the first dynode. The bleaching radiation was focused onto the sample through the microscope objective using a small laboratory microscope modified for epifluorescence. The observation beam was the 514.6-nm line of a Spectra-Physics 164-05 Argon ion laser (Spectra-Physics, Inc., Mountain View, Calif.), and was directed onto the sample without any focusing of the beam. Electronics were constructed to control the timing of the bleach pulse and gating circuit, as well as to amplify the phototube output. The signal was detected on a fast-storage oscilloscope (HP 1774A; Hewlett-Packard Co., Palo Alto, Calif.) and recorded on Polaroid film (Polaroid Corp. Cambridge, Mass.)

It was discovered in these initial experiments that the observed rotation times were much longer than expected, and could in fact be conveniently measured with minor modifications of the pattern photobleaching apparatus already in use in this laboratory. Unless otherwise noted, all measurements reported here were made with the latter apparatus. (The two experimental arrangements gave comparable results.) This apparatus is briefly described below.

A block diagram is shown in Fig. 2. The beam (514.6 nm) from a Spectra-Physics 164–05 Argon ion laser is directed into a beam splitter using only 90° reflections from mirrors to avoid depolarization of the light. It is then divided and recombined using two 10% beam splitters to give two independently controlled beams of different intensities traveling along the same optical axis. The beam is directed into

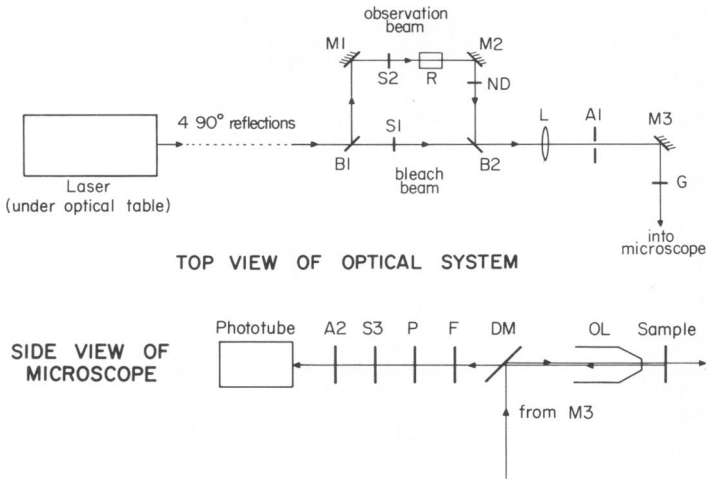

FIGURE 2 Simplified block diagram of the optical system used in rotation measurements. B1, B2, 10% beamsplitters; M1, M2, M3, front surface mirrors; S1, S2, S3, electronic shutters (Uniblitz); R, Spectra Physics 310A polarization rotator; ND, neutral density filter(s); L, optional focusing lens ($f \simeq 50$ cm); A1, variable iris diaphragm; G, optional Ronchi ruling for translational diffusion measurements; OL, microscope objective lens (planachromat, air, NA = 0.65); DM, dichroic mirror FT 580 (Zeiss); F, interference filter LP 590 (Zeiss); P, observation polarizer; A2, fixed aperture.

the rear of an epifluorescence microscope (Zeiss Photomicroscope III; Carl Zeiss, Inc., New York) and focused by the microscope optics onto the sample. The excited fluorescence is detected with a cooled phototube (RCA C31034-02) mounted on the microscope. The polarization of the exciting beam at the sample is >95%, as determined by measurements on the beam after passage through the objective. The divergence of the exciting beam at the sample is small, <5°. In the experiments reported in this paper the numerical aperture of the objective lens is 0.65. The beam may be further focused if desired using a single long focal length (~50 cm) lens placed in the beam near the microscope. For rotation measurements a polarization rotator (Spectra-Physics 310A) is placed in the observation beam path before recombination with the bleach beam. A linear polarizer either parallel or perpendicular to the observation beam polarization is placed in the microscope above the sample so that only one polarization of the emitted fluorescence is detected by the phototube.

The sequence of events in a rotation measurement is as follows. The liposome or multibilayer sample is focused in the microscope field of view. The desired polarizations of the observation beam and the detector polarizer are selected. The observation beam is attenuated with neutral density filters to give an appropriate fluorescence intensity for measurement using the phototube. The amplified phototube output is displayed on a storage oscilloscope and the oscilloscope gain set to give a full-scale initial intensity level. At the beginning of the experiment there is a bleach pulse followed by an observation beam (which is chopped for experiments with a time scale greater than several seconds) for measuring the fluorescence intensity. The data are recorded on the storage oscilloscope and simultaneously sent to a computer (PDP 8/E; Digital Equipment Corp.; Maynard, Mass.) for storage and analysis. The data are fit to a single exponential to give the fluorescence recovery time constants recorded.

THEORY

In this section we use a simple set of assumptions to calculate the fluorescence recovery that follows photobleaching and results from uniaxial rotational diffusion of a fluorescent membrane component. The calculations are first kept in general form to show the potential

applicability of the method to complex systems such as proteins labeled with fluorescence. The calculations are then simplified to account for our experimental studies of the rotational diffusion of the lipid probe diI in lipid bilayer membranes. An alternative treatment of rotational motion may be found in the Appendix.

Spherical Membrane

DEFINITION OF AXES The laboratory (microscope)-fixed axis system is designated by the unit vectors $\mathbf{i}'$, $\mathbf{j}'$, $\mathbf{k}'$. The direction of polarization of the bleach-burst radiation is *always* taken to be $\mathbf{k}'$. The optical axis of the microscope, which is the direction of propagation of the laser radiation, is always taken to be $\mathbf{j}'$. The probe excitation beam is sometimes polarized along $\mathbf{k}'$ and sometimes polarized along $\mathbf{i}'$. The fluorescent molecule-fixed axis system, $\mathbf{i}$, $\mathbf{j}$, $\mathbf{k}$ is used to describe the orientation of the electronic absorption and emission dipoles (taken to be parallel), $\boldsymbol{\mu}$. This axis system is chosen so that $\boldsymbol{\mu}$ lies in the plane of $\mathbf{i}$ and $\mathbf{k}$.

$$\boldsymbol{\mu} = \mu_i \mathbf{i} + \mu_k \mathbf{k} \tag{1}$$

(For consideration of a related problem where the absorption and emission dipoles are not parallel, see Axelrod, 1979.) These axis systems are shown in Fig. 3. The vector $\mathbf{k}$ is normal to the tangent plane of the spherical membrane, and is assumed to be the axis of rotation of the membrane-bound fluorescent molecule. The location of the fluorescent molecule on the membrane surface is given by the polar angles θ, ϕ and the orientation of the $\mathbf{i}$, $\mathbf{j}$, $\mathbf{k}$ axis system relative to the $\mathbf{i}'$, $\mathbf{j}'$, $\mathbf{k}'$ axis system is given by the Euler angles α, β, γ.

Note that because $\mathbf{k} \cdot \mathbf{k}' = \cos\theta = \cos\beta$, it follows that $\theta = \beta$. Also $\mathbf{i}' \cdot \mathbf{k} = \sin\alpha \sin\beta = \cos\phi \sin\theta$ so α and ϕ only differ by $\pi/2$ and thus represent equivalent rotations. The angle γ represents the pure axial rotation of the fluorescent molecule and, before photobleaching, all values of γ are assumed to be equally probable.

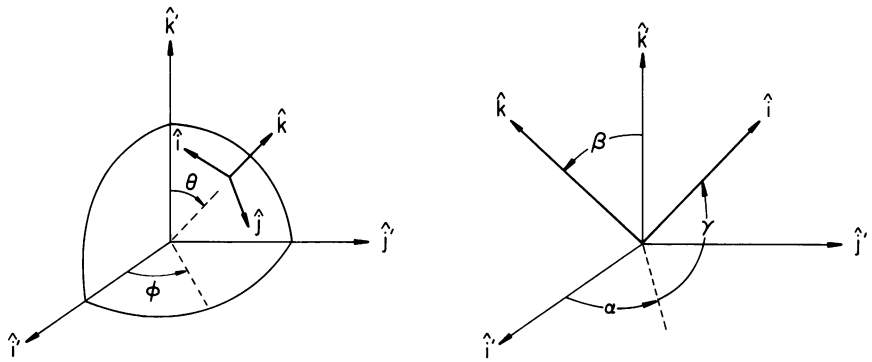

FIGURE 3 Laboratory (microscope)- and molecule-fixed axis systems, $\mathbf{i}'$, $\mathbf{j}'$, $\mathbf{k}'$ and $\mathbf{i}$, $\mathbf{j}$, $\mathbf{k}$, respectively. The location of the membrane-bound fluorescent molecule is given by the polar angles θ, ϕ and the orientation of the $\mathbf{i}$, $\mathbf{j}$, $\mathbf{k}$ axis system relative to the $\mathbf{i}'$, $\mathbf{j}'$, $\mathbf{k}'$ axis system is given by the Euler angles α, β, γ. The latter angles are generated as follows. Start with $\mathbf{i} = \mathbf{i}'$, $\mathbf{j} = \mathbf{j}'$, $\mathbf{k} = \mathbf{k}'$. Rotate $\mathbf{i}$ towards $\mathbf{j}'$ about $\mathbf{k}'$ by the angle α. Rotate $\mathbf{k}$ away from $\mathbf{k}'$ about $\mathbf{i}$ by the angle β. Finally rotate $\mathbf{i}$ away from its intermediate position to its final position by a rotation of γ about the axis $\mathbf{k}$.

Photobleaching Recovery

We now let $\rho(\alpha, \beta, \gamma, t)$ be the probability that a fluorescent transition dipole μ have the orientation α, β, γ at time t. $\rho(\alpha, \beta, \gamma, t, <-\Delta t)$ is the orientation probability distribution before the bleach pulse. By assumption, this does not depend on α or γ, and the dependence on β is proportional to $\sin \beta$:

$$\rho(\alpha, \beta, \gamma, t<-\Delta t) = \rho_0 \sin \beta \tag{2}$$

where ρ_0 is a constant. The bleach burst lasts during the period $-\Delta t < t < 0$. All the bleaching radiation has the same polarization, $\mathbf{k}'$, so that the linear probability of photon absorption is proportional to $(\boldsymbol{\mu} \cdot \mathbf{k}')^2$. Thus, if the photobleaching is weak (linear) the number of remaining fluorescent molecules at α, β, γ is proportional to the number initially present at α, β, γ (i.e., $\rho_0 \sin \beta$) minus the number bleached at α, β, γ:

$$\rho(\alpha, \beta, \gamma, t = 0) = [\rho_0 - \lambda(\boldsymbol{\mu} \cdot \mathbf{k}')^2] \sin \beta. \tag{3}$$

Here λ is a constant, proportional to ρ_0, the bleach radiation intensity, the duration of the very short bleach (Δt), and fundamental constants. In terms of the Euler angles α, β, γ,

$$\begin{aligned}(\boldsymbol{\mu} \cdot \mathbf{k}')^2 &= [\mu_i \sin \gamma \sin \beta + \mu_k \cos \beta]^2 \\ &= \mu_k^2 \cos^2 \beta + 2\,\mu_i \mu_k \sin \gamma \sin \beta \cos \beta \\ &\quad + \tfrac{1}{2}\,\mu_i^2 (1 - \cos 2\gamma) \sin^2 \beta.\end{aligned} \tag{4}$$

We now consider the orientational probability distribution for molecules after the bleach burst, $\rho(\alpha, \beta, \gamma, t > 0)$. If we assume that no translational diffusion takes place during the observation time, the ρ changes with time only through its dependence on γ. Thus for $t > 0$, $\rho(\alpha, \beta, \gamma\, t)$ must satisfy the rotational diffusion equation,

$$\tau(\partial\rho/\partial t) = \partial^2\rho/\partial\gamma^2 \tag{5}$$

subject to the boundary conditions that $\rho(\alpha, \beta, \gamma, 0)$ is given by Eq. 3, and $\rho(\alpha, \beta, \gamma, \infty)$ is independent of γ. Here τ is the rotation time constant.

The "normal mode" solutions to the diffusion equation for rotation are

$$\sin m\gamma e^{-m^2 t/\tau} \tag{6}$$

$$\cos m\gamma e^{-m^2 t/\tau} \tag{7}$$

where $m = 0, 1, 2\ldots$ Using these solutions of the diffusion equation we can immediately write down the solution for $\rho(\alpha, \beta, \gamma, t)$ for $t > 0$ that satisfies the two boundary conditions:

$$\begin{aligned}\rho(\alpha, \beta, t) = \rho_0 \sin \beta &- \gamma[\mu_k^2 \cos^2 \beta \\ &+ 2\mu_i \mu_k \sin \beta \cos \beta \sin \gamma\, e^{-t/\tau} \\ &+ \tfrac{1}{2}\,\mu_i^2 (1 - \cos 2\gamma\, e^{-4t/\tau}) \sin^2 \beta] \sin \beta.\end{aligned} \tag{8}$$

In the present work we are concerned with the experimental determination of the rotation

time constant τ, and to begin with, will only calculate $\rho_t(\alpha, \beta, \gamma, t)$, the time-dependent part of $\rho(\alpha, \beta, \gamma, t)$:

$$-1/\lambda\, \rho_t(\alpha, \beta, \gamma, t) = 2\mu_i\mu_k \sin^2\beta \cos\beta \sin\gamma\, e^{-t/\tau} - \tfrac{1}{2}\mu_i^2 \sin^3\beta \cos 2\gamma e^{-4t/\tau}. \tag{9}$$

The symbol ρ_c is used later for the time-independent part of ρ that is proportional to λ. We now calculate a quantity $P'_{\parallel}(\alpha, \beta, \gamma, t)$ that is proportional to the time-dependent fluorescent emission of molecules having the orientation α, β, γ when excited by a probe beam having the polarization $\mathbf{k}'$.

$$P'_{\parallel}(\alpha, \beta, \gamma, t) = (\boldsymbol{\mu} \cdot \mathbf{k}')^2 \rho_t. \tag{10}$$

Similarly, when the probe beam has an orientation perpendicular to the bleach beam, the time-dependent fluorescence emission is proportional to

$$P'_{\perp}(\alpha, \beta, \gamma, t) = (\boldsymbol{\mu} \cdot \mathbf{i}')^2 \rho_t \tag{11}$$

We now average $P'_{\parallel}$ and $P'_{\perp}$ over all angles α, β and γ to obtain $\overline{P'_{\parallel}}$ and $\overline{P'_{\perp}}$, quantities proportional to the number of fluorescent photons emitted in the two cases.

For example,

$$\overline{P'_{\parallel}} = \frac{1}{4\pi^3} \int_0^{2\pi} \int_0^{\pi} \int_0^{2\pi} d\alpha\, d\beta\, d\gamma\, P'_{\parallel}(\alpha, \beta, \gamma, t). \tag{12}$$

These integrations yield

$$\overline{P'_{\parallel}} = [-14\lambda\mu_i^4/210] f_3(t) \tag{13}$$

$$\overline{P'_{\perp}} = [7\lambda\mu_i^4/210] f_3(t) \tag{14}$$

where

$$f_3(t) = (4 \tan^2 \epsilon e^{-t/\tau} + e^{-4t/\tau}) \tag{15}$$

and

$$\tan \epsilon = \mu_k/\mu_i. \tag{16}$$

The two expressions for $\overline{P'_{\parallel}}$ and $\overline{P'_{\perp}}$ represent fluorescence recoveries and decays, respectively, with relative amplitudes that differ by a factor of two. The above results have two important properties. First, unless $\epsilon = 0$, two time constants are involved in the fluorescence recoveries. Second, the above results are easily generalized to allow for several transition dipole moments to be located at each point θ, ϕ on the surface of the spherical lipid vesicle (or cell). A multiplicity of fluorophores in a given surface region will in general enhance the recovery amplitude, since the recovery amplitudes have the same sign and are always additive.

Polarization of the Emitted Radiation

FINITE APERTURE OBSERVATION In this section the effect of the finite aperture of the microscope objective lens in collecting fluorescent radiation is considered. It is not

necessary to consider the effect of a finite aperture on the bleaching radiation since direct measurements of the divergence of the laser beam at the sample shows this divergence to be small (<5°). In this section we also treat the effect of placing a polarizer between the sample and the phototube. Eqs. 13 and 14 are proportional to the total emitted radiation from a spherical sample, and this is proportional to the radiation detected by a microscope objective lens with a numerical aperture of one. One can use the equations derived by Axelrod (1979) to calculate the intensity and polarization of the radiation detected by a lens with finite aperture. For a single, uniquely oriented transition dipole moment μ in the sample, the radiation emitted parallel and perpendicular to the probe beam having polarization ($\mathbf{m}' = \mathbf{k}'$ or $\mathbf{i}'$) is proportional to

$$I_{\parallel} = 1/\mu^2 [K_a(\mu \cdot \mathbf{j}')^2 + K_b(\mu \cdot \mathbf{n}')^2 + K_c(\mu \cdot \mathbf{m}')^2] \tag{17}$$

$$I_{\perp} = 1/\mu^2 [K_a(\mu \cdot \mathbf{j}')^2 + k_c(\mu \cdot \mathbf{n}')^2 + K_b(\mu \cdot \mathbf{m}')^2]. \tag{18}$$

When the polarizer in front of the phototube transmits light parallel (perpendicular) to the probe beam polarization, the detected light has intensity $I_{\parallel}$ ($I_{\perp}$). The probe beam itself may have a polarization parallel (perpendicular) to the bleach beam, $\mathbf{m}' = \mathbf{k}'$ ($\mathbf{m}' = \mathbf{i}'$).

In Eqs. 17 and 18 $\mathbf{n}'$ is a unit vector perpendicular to $\mathbf{m}'$ and $\mathbf{j}'$. Here, from Axelrod (1979):

$$K_a = 1/3(2 - 3\cos\sigma_0 + \cos^3\sigma_0) \tag{19}$$

$$K_b = 1/12(1 - 3\cos\sigma_0 + 3\cos^2\sigma_0 - \cos^3\sigma_0) \tag{20}$$

$$K_c = 1/4(5 - 3\cos\sigma_0 - \cos^2\sigma_0 - \cos^3\sigma_0). \tag{21}$$

The numerical aperture (in air) is $\sin\sigma_0$. It is convenient to rewrite Eqs. 17 and 18 as follows:

$$I_{\parallel} = K_a + 1/\mu^2[K_{ba}(\mu \cdot \mathbf{n}')^2 + K_{ca}(\mu \cdot \mathbf{m}')^2] \tag{22}$$

$$I_{\perp} = K_a + 1/\mu^2[K_{ca}(\mu \cdot \mathbf{n}')^2 + K_{ba}(\mu \cdot \mathbf{m}')^2] \tag{23}$$

where $K_{ba} = K_b - K_a$, $K_{ca} = K_c - K_a$ and $\mu^2 = (\mu \cdot \mathbf{j}')^2 + (\mu \cdot \mathbf{m}')^2 + (\mu \cdot \mathbf{n}')^2$. In the experiments reported here the probe-beam polarization is either parallel or perpendicular to the bleach-beam polarization, and also either parallel or perpendicular to the polarization direction of the polarizer in front of the phototube. This gives four different experimental configurations: bleach $\parallel$ probe $\parallel$ observation ($\parallel$, $\parallel$); bleach $\parallel$ probe $\perp$ observation ($\parallel$, $\perp$); etc.

To calculate quantities proportional to the time-dependent detected fluorescence for each of these configurations, Eqs. 22 and 23 must be multiplied by the distribution probabilities ρ_t, by the probe-beam excitation probabilities (proportional to $[\mu \cdot \mathbf{k}']^2$ or $[\mu \cdot \mathbf{i}']^2$), and then averaged over α, β and γ for the different orientations.

$$\bar{I}(\parallel, \parallel) = K_a\overline{\rho_t(\mu \cdot \mathbf{k}')^2} + 1/\mu^2[K_{ba}\overline{\rho_t(\mu \cdot \mathbf{i}')^2(\mu \cdot \mathbf{k}')^2} + K_{ca}\overline{\rho_t(\mu \cdot \mathbf{k}')^4}]. \tag{24}$$

$$\bar{I}(\parallel, \perp) = K_a\overline{\rho_t(\mu \cdot \mathbf{k}')^2} + 1/\mu^2[K_{ca}\overline{\rho_t(\mu \cdot \mathbf{k}')^2(\mu \cdot \mathbf{i}')^2} + K_{ba}\overline{\rho_t(\mu \cdot \mathbf{k}')^4}]. \tag{25}$$

$$\bar{I}(\perp, \parallel) = K_a\overline{\rho_t(\mu \cdot \mathbf{i}')^2} + 1/\mu^2[K_{ba}\overline{\rho_t(\mu \cdot \mathbf{i}')^2(\mu \cdot \mathbf{k}')^2} + K_{ca}\overline{\rho_t(\mu \cdot \mathbf{i}')^4}]. \tag{26}$$

$$\bar{I}(\perp, \perp) = K_a\overline{\rho_t(\mu \cdot \mathbf{i}')^2} + 1/\mu^2[K_{ca}\overline{\rho_t(\mu \cdot \mathbf{i}')^2(\mu \cdot \mathbf{k}')^2} + K_{ba}\overline{\rho_t(\mu \cdot \mathbf{i}')^4}]. \tag{27}$$

In the above equations,

$$\overline{\rho_t(\mu \cdot \mathbf{k}')^2} = (-14\lambda/210)[\mu_i^4 f_3(t)] \tag{28}$$

$$\overline{\rho_t(\mu \cdot \mathbf{i}')^2} = (7\lambda/210)[\mu_i^4 f_3(t)] \tag{29}$$

$$\overline{\rho_t(\mu \cdot \mathbf{k}')^4} = (-12\lambda/210)[\mu^2\mu_i^4 f_3(t)] \tag{30}$$

$$\overline{\rho_t(\mu \cdot \mathbf{k}')^2(\mu \cdot \mathbf{i}')^2} = (-\lambda/210)[(1 + 3\cos^2\epsilon)\mu^2\mu_i^4 f_3(t)] \tag{31}$$

$$\overline{\rho_t(\mu \cdot \mathbf{i}')^4} = (6\lambda/210)[\mu^2\mu_i^4 f_3(t)]. \tag{32}$$

It may be noted that all terms in the fluorescence recoveries (or decays) have the same time dependence, $f_3(t)$. If an analysis of an observed time dependence could be resolved into two time-dependent exponentials, then the relative values of μ_i^2 and μ_k^2 could be obtained. Note also that for a numerical aperture of one, $K_a = 2/3$, $K_{ba} = -7/12$; $K_{ca} = 7/12$; the sum of Eqs. 24 and 25 is proportional to $\overline{P'_\parallel}$ (Eq. 13); and the sum of Eqs. 26 and 27 is proportional to $\overline{P'_\perp}$ (Eq. 14), as expected. The fact that these quantities are not identical is simply related to the absolute magnitude of K_a chosen by Axelrod (1979).

For our experiments (see below) we used a microscope objective lens with a numerical aperture of 0.65 (air), for which $K_a = 0.053020$, $K_{ba} = -0.051865$, and $K_{ca} = 0.372945$. These values adequately approximate the low-aperture limit $|K_c| \gg |K_a|, |K_b|$. We have not made corrections for a finite aperture in the present paper since these corrections are comparable to or less than the experimental error. Thus, in the following calculations we have neglected K_a, and K_{ba} in Eqs. 24–27. The magnitude of K_{ca} is then irrelevant because it cancels in the subsequent calculations of fluorescence intensity ratios. We have included the aperture corrections in the present paper since it is likely they will be needed in future work.

Two-Dimensional Case (Coplanar Phospholipid Multibilayers)

The case where the bleach and probe radiation propagates perpendicular to the planes of coplanar multibilayer membranes can be derived from the three-dimensional cases by fixing the Euler angles $\alpha = 0$ and $\beta = \pi/2$ (cf. Eqs. 2–4). Thus, for the two-dimensional case

$$\rho_t(\gamma, t) = (\lambda/2)\mu_i^2 \cos 2\gamma f_2(t) \tag{33}$$

$$(\mu \cdot \mathbf{k}')^2 = 1/2\mu_i^2(1 - \cos 2\gamma) \tag{34}$$

$$(\mu \cdot \mathbf{i}')^2 = 1/2\mu_i^2(1 + \cos 2\gamma) \tag{35}$$

where

$$f_2(t) = e^{-4t/\tau}. \tag{36}$$

For this two-dimensional case one then obtains the following equations:

$$\mu^2\overline{\rho_t(\mu \cdot \mathbf{k}')^2} = -1/8\lambda\mu^2\mu_i^4 f_2(t) \tag{37}$$

$$\mu^2\overline{\rho_t(\mu \cdot \mathbf{i}')^2} = 1/8\lambda\mu^2\mu_i^4 f_2(t) \tag{38}$$

$$\overline{\rho_t(\mu \cdot \mathbf{k}')^4} = -1/8\lambda\mu_i^6 f_2(t) \tag{39}$$

$$\overline{\rho_t(\mu \cdot \mathbf{i}')^4} = -1/8\lambda\mu_i^6 f_2(t) \tag{40}$$

$$\overline{\rho_t(\mu \cdot \mathbf{i}')^2(\mu \cdot \mathbf{k}')^2} = 0. \tag{41}$$

For the two-dimensional sample, only a single recovery time $\sigma = \tau/4$ is expected, for the recovery (or decay) curves. We will discuss these equations further in connection with our experimental results.

Recovery/Bleach Ratios

A quantity that is convenient in the analysis of the experimental data is the recovery/bleach ratio R:

$$R = (I_3 - I_2)/(I_1 - I_2). \tag{42}$$

Here I_1, I_2, and I_3 are the intensities of fluorescent radiation detected by the phototube before photobleaching ($t < -\Delta t$) immediately after photobleaching ($t = 0$) and after complete recovery ($t = \infty$), respectively. Thus, $I_3 - I_2$ is a measure of the recovery amplitude and $I_1 - I_2$ is a measure of the bleach amplitude. Under the assumptions of our calculation, theoretical values of R are independent of λ for small λ (weak bleaching), and are independent of the probe beam intensity for nonbleaching probe beam intensities. Also, for the various experimental configurations used, e.g., $R(\parallel, \parallel)$, $R(\perp, \parallel)$, etc., the experimental values of R should be independent of a polarization-dependent sensitivity in the detection system following the observation polarizer.

In the low-aperture limit the recovery amplitude $I_3 - I_2$ for the $(\parallel, \parallel)$ case is proportional to $[\rho_t(0)](\mu \cdot \mathbf{k}')^4$ where $\rho_t(0)$ is the value of ρ_t at time $t = 0$. The bleach amplitude, $I_1 - I_2$ for the $(\parallel, \parallel)$ case is $\{\rho_c + \rho_t(0)\}(\mu \cdot \mathbf{k}')^4$. Thus, we obtain the following expression for $R(\parallel, \parallel)$.

$$R(\parallel, \parallel) = \overline{\rho_t(0)(\mu \cdot \mathbf{k}')^4}/\overline{\{\rho_c + \rho_t(0)\}(\mu \cdot \mathbf{k}')^4}. \tag{43}$$

Similar expressions can be derived for $R(\parallel, \perp)$, etc. The following Eqs. 44–48 give calculated expressions for $\rho_c(\mu \cdot \mathbf{k}')^4$, $\rho_c(\mu \cdot \mathbf{i}')^4$, etc. For brevity, these expressions are shown only for the special case $\epsilon = 0$. These results are used to calculate the theoretical values of R for comparison with experimental values.

For the three-dimensional (spherical) case when $\epsilon = 0$,

$$\mu^2\overline{\rho_c(\mu \cdot \mathbf{k}')^2} = (-28\lambda/210)\mu_i^6 \tag{44}$$

$$\mu^2\overline{\rho_c(\mu \cdot \mathbf{i}')^2} = (-21\lambda/210)\mu_i^6 \tag{45}$$

$$\overline{\rho_c(\mu \cdot \mathbf{k}')^4} = (-18\lambda/210)\mu_i^6 \tag{46}$$

$$\overline{\rho_c(\mu \cdot \mathbf{i}')^2(\mu \cdot \mathbf{k}')^2} = (-5\lambda/210)\mu_i^6 \tag{47}$$

$$\overline{\rho_c(\mu \cdot \mathbf{i}')^4} = (-12\lambda/210)\mu_i^6 \tag{48}$$

and for the two-dimensional (multibilayer) case

$$\mu^2\overline{\rho_c(\mu \cdot \mathbf{k}')^2} = (-\lambda/4)\mu_i^6 \tag{49}$$

$$\mu^2\overline{\rho_c(\mu \cdot \mathbf{i}')^2} = (-\lambda/4)\mu_i^6 \tag{50}$$

$$\overline{\rho_c(\mu \cdot \mathbf{k}')^4} = (-3\lambda/16)\mu_i^6 \tag{51}$$

$$\overline{\rho_c(\mu \cdot \mathbf{i}')^2(\mu \cdot \mathbf{k}')^2} = (-\lambda/16)\mu_i^6 \tag{52}$$

$$\overline{\rho_c(\mu \cdot \mathbf{i}')^4} = (-3\lambda/16)\mu_i^6. \tag{53}$$

TABLE I
RECOVERY/BLEACH RATIOS

	Theoretical*	Experimental
Two Dimensions (coplanar multibilayers)‡		
$R(\parallel, \parallel)$	0.40	0.49 ± 0.1
$R(\perp, \parallel)$	−2.00	−1.93 ± 0.11
$R(\parallel, \perp)$	0	0.13 ± 0.01
$R(\perp, \perp)$	0	0.17 ± 0.03
Three Dimensions (spherical liposome)‡§		
$R(\parallel, \parallel)$	0.40	0.39 ± 0.03
$R(\perp, \parallel)$	−1.00	−0.68 ± 0.15
$R(\parallel, \perp)$	0.44	0.28 ± 0.04
$R(\perp, \perp)$	0.44	0.31 ± 0.03

*Theoretical calculations assume that the lipid probe is oriented in the membrane so that the transition dipole for absorption and emission are parallel and in the plane of the membrane, $\epsilon = 0$.
‡96 mol % DSPC and 4 mol % cholesterol. Uncertainties are standard errors of the means.
§Measurements on liposomes were made using a focused beam width of several liposome diameters. See text.

Theoretical bleach/recovery ratios are given in Table I. The theoretical values apply to the low-aperture limit.

RESULTS

Fig. 4 shows representative fluorescence recovery and decay curves for the lipid probe dil (0.005 mol %) in coplanar multibilayer membranes containing 4 mol % cholesterol and 96 mol % DSPC. The fluorescence intensity of 100 refers to the intensity recorded before bleaching using the probe beam (see Experimental). The fluorescence recovery and decay curves correspond to the polarization directions, bleach $\parallel$ probe $\parallel$ observed (obs), and bleach $\perp$ probe $\parallel$ obs, respectively. The values of the recovery/bleach amplitude ratios R obtained from the two curves are $R(\parallel, \parallel) = 0.5$ and $R(\perp, \parallel) = -2.0$. Theoretical and average expeimental ratios are given in Table I for both coplanar multibilayers and liposomes. Liposomes had diameters typically in the 10–20-μm range. Fig. 5 gives representative recovery and decay curves for multilamellar liposomes composed of pure DSPC and 0.005 mol % dil. Experimental values of R for these curves are given in the figure legend. Average values of R for liposomes are given in Table I. As discussed later, deviations between observed and theoretical R values can arise for a number of reasons, including overbleaching, bilayer geometry, and fluorescence depolarization. Discrepancies between observed and theoretical ratios in Table I may arise from all of these sources.

Values of the measured recovery time constants σ are shown as a function of temperature in Fig. 6 for both coplanar multibilayer membranes and multilamellar liposomes. The lipid compositions vary between pure DSPC and 80 mol % DSPC, 20 mol % cholesterol. Data for DPPC and DPPC-cholesterol multibilayer membranes are also given in this figure. For a given lipid composition and temperature, values of σ are independent of membrane geometry (planar or spherical) to within the experimental error. Calculated "activation energies" for rotational diffusion are ~33 kcal/mol.

We have carried out studies of translational diffusion in parallel with the studies of

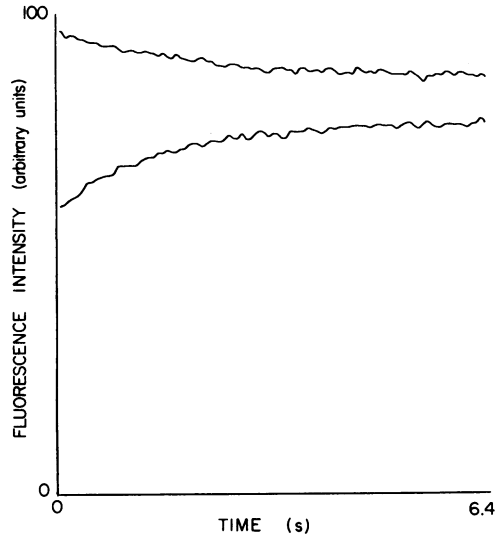

FIGURE 4 Representative fluorescence recovery and decay curves from a DSPC, 4% cholesterol oriented multibilayer membrane containing 0.005 mol % dil, at room temperature. The recovery curve is for the experimental configuration bleach ∥ probe ∥ obs (see Theory section for an explanation of this terminology). The total scan time in this figure is 6.4 s. The decay curve is for the experimental configuration bleach ⊥ probe ∥ obs. Measured values of R from these curves are $R(\parallel, \parallel) = 0.5$, $R(\perp, \parallel) = -1.93$. The recovery time constants σ are $(\parallel, \parallel) = 0.74$ s, $(\perp, \parallel) = 0.99$ s.

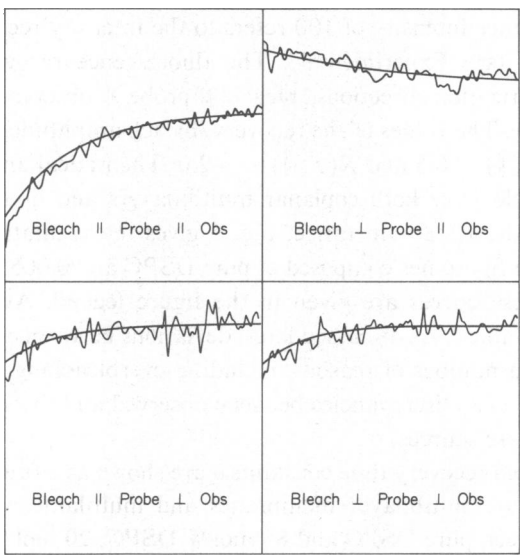

FIGURE 5 Representative fluorescence recovery and decay curves obtained from multilamellar liposomes of DSPC containing 0.005 mol % dil. Measured values of R from these curves are $R(\parallel, \parallel) = 0.43$, $R(\parallel, \perp) = 0.25$, $R(\perp, \parallel) = -0.50$, $R(\perp, \perp) = 0.38$. The total scan time is 320 ms. The vertical axes are 80% (baseline) to 100% (full scale) of prebleach fluorescence intensity.

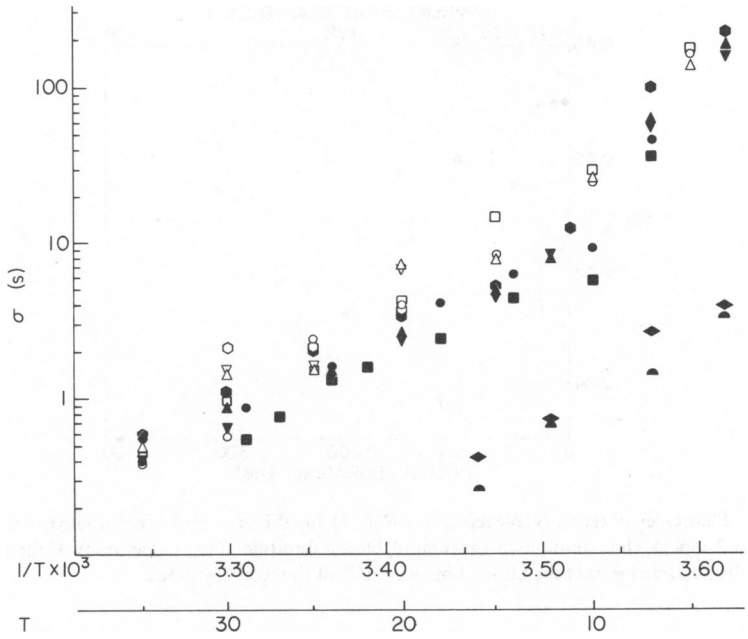

FIGURE 6 Temperature dependence of experimental values for the rotation recovery times for dil in liposomes and coplanar multibilayers. Multilayers of DSPC containing various molar concentrations of cholesterol: ● (0%), ■ (5%), ▲ (10%), ▼ (15%), ⬢ (20%). Liposomes of DSPC containing various molar concentrations of cholesterol: ○ (0%), □ (5%), △ (10%), ▽ (15%), ⬡ (20%). Multilayers of DPPC containing various molar concentrations of cholesterol ♦ (10%), ⬬ (15%). Units: $1/T \times 10^3$ (degree^{-1}); T (degree C).

rotational diffusion reported above. Translational diffusion was measured using pattern photobleach-recovery methods (Smith and McConnell, 1978; Smith et al., 1979). Typical recovery times were >2h, for a stripe spatial period of the order of 5 μm, corresponding to lateral diffusion coefficients of 10^{-12} cm^2/s or less. These results show that our photobleach-recovery curves without a grid cannot be due to lateral diffusion.

Under some conditions of temperature and lipid membrane composition a light-induced increase in fluorescence intensity is observed. That is, immediately upon illuminating the sample with a low intensity (100 mW/cm^2) observation beam a time-dependent increase in fluorescence intensity is observed, on a time scale comparable to the time scale of rotation. This phenomenon interferes with measurements of rotation, as it introduces an additional time-dependent change in fluorescence intensity. Therefore, in all cases where this phenomenon was observed we either (*a*) chopped the observation beam with a sufficiently short on-time that no photo-induced increase in fluorescence intensity occurs during the measurements, or (*b*) held a continuous observation beam on the sample before and after bleaching to saturate the change in fluorescence intensity.

In the case of liposomes, observed recovery/bleach ratios depend on the extent to which the bleaching beam is focused; if the beam is centered and focused to a half-width comparable to or less than the diameter of a liposome, the observed recovery/bleach ratios approach those of

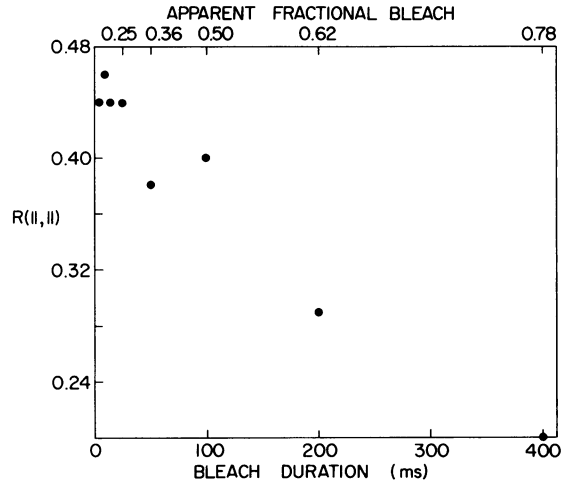

FIGURE 7 Fluorescence recovery/bleach ratios $R(\parallel, \parallel)$ for dil in coplanar multibilayers composed of DSPC with 2 mol % cholesterol, as a function of bleach duration. The temperature of the experiment (11–18°C) was selected so that the bleach time was ≤5% of the recovery time σ.

coplanar multibilayers. Thus, to compare the calculated and observed recovery/bleach ratios for liposomes we have used a beam width significantly larger than the liposome diameter.

Fig. 7 shows measured values of $R(\parallel, \parallel)$ for multibilayers (2% cholesterol in DSPC) as a function of the bleach duration. As expected, the absolute magnitudes of R decrease with increasing bleach. It will be seen that the peak value for $R(\parallel, \parallel)$ is only approached for short bleaches, 0–25 ms, corresponding to bleaches of <25%. In principle, such plots permit an extrapolation to zero bleach, although this procedure has not been used in the present work in reporting R values in Table I.

An additional check on the approximations used in the theoretical calculations can be made by comparing measured fractional bleaches I_2/I_1 for various experimental configurations. For a given radiation intensity and time of bleaching (well within the linear bleaching time regime, <15% bleach for $(\parallel, \parallel)$), we have observed relative bleach ratios of 1, 0.98, 0.3, 1.05 (0.005 mol % dil in liposomes of DSPC, 4% cholesterol). Calculated values are 1, 0.90. 0.20, and 0.90.

All of the above calculated fluorescence intensities have assumed that there is no intrinsic depolarization of fluorescence except that due to the (slow) molecular rotation itself. To check this assumption we have measured various fluorescence intensity (F) ratios (no bleaching), with the following typical results for liposomes.

$$F(\parallel, \parallel)/F(\parallel, \perp) = 2.8 \tag{54}$$

$$F(\perp, \parallel)/F(\perp, \perp) = 1.5 \tag{55}$$

and for multilayers

$$F(\parallel, \parallel)/F(\parallel, \perp) = 3.27 \tag{56}$$

$$F(\perp, \parallel)/F(\perp, \perp) = 2.06. \tag{57}$$

The ratios in Eqs. 54 and 55 (as well as Eqs. 56 and 57) are not equal due to a polarization sensitivity of the detection system. In experiments with dil fluorescence excited by an unpolarized light source (UV lamp) we measured a detection sensitivity anisotropy of $\eta = 1.3$ such that light polarized in the direction $\mathbf{k}'$ was detected with higher sensitivity. Estimates of the detection anisotropy factor η and the intrinsic fluorescence polarization factor δ may also be obtained directly from the data in Eqs. 54–57. For the first two equations, we set $\eta\delta = 2.8$, $\delta/\eta = 1.5$, from which $\eta = 1.4$, $\delta = 2.1$. From Eqs. 56 and 57, $\eta\delta = 3.27$ and $\delta/\eta = 2.06$; thus $\eta = 1.26$ and $\delta = 2.6$.

From these results it is clear that our detection system has a polarization sensitivity and that the fluorescence emission of dil is somewhat depolarized. If there is no fluorescence depolarization, the polarization factor would be equal to three for both multilayers and liposomes. The instrumental anisotropy should not contribute to the experimental recovery/bleach ratios. Fluorescence depolarization can affect some of these ratios. When a simple calculation is used to correct the calculated recovery/bleach ratios for depolarization it is found that these corrections are within our experimental errors. Fluorescence depolarization does not affect the calculated values for $R(\parallel, \perp) = R(\perp, \perp) = 0$ in the case of coplanar multibilayers. The above calculations as well as the comparison in Table I suggest that the theoretical analysis of the data is more reliable for the coplanar multibilayers. For the coplanar multibilayers our depolarization factor is the same as that reported by Ygueribide and Stryer (1971). The deviations of liposomes from spherical shapes may account for the larger discrepancies between theory and experiment in this case.

DISCUSSION

The agreement between the theoretical and experimental results, especially the recovery/bleach ratios in Table I, provide compelling evidence that (*a*) the observed fluorescence recovery and decay curves do provide a measure of rotational diffusion, and (*b*) the assumptions and approximations used in the theoretical analysis are adequate. The special assumption, that the transition dipole moment lies in the plane of the membrane ($\epsilon = 0$) is further supported by the observation that the same recovery times are measured for liposomes and coplanar multilayers. [Compare $f_3(t)$ and $f_2(t)$ in Eqs. 15 and 36.] The assumption $\epsilon = 0$ is also in qualitative accord with direct visual observation using polarized light, where it is observed that the spatial distribution of fluorescence intensity is nonuniform over the surface of the liposomes. For a quantitative discussion of a closely related problem, see Axelrod (1979).

The possible contribution of lateral diffusion to the recovery curves has been ruled out by direct measurements of the lateral diffusion (see Results). The negative recoveries $R(\perp, \parallel)$ rule out photochemical recovery.

To achieve the satisfactory agreement between theory and experiment seen in Table I it is necessary to use weak bleach amplitudes (cf. Fig. 7). This of course is related to the use of the linear approximation, Eq. 3. If the bleach were not weak, Eq. 3 would have to be replaced by an exponential dependence of the distribution function $\rho(\alpha, \beta, \gamma, t = 0)$ on λ:

$$\rho(\alpha, \beta, \gamma, t = 0) = \rho_0 \exp - [\lambda(\boldsymbol{\mu} \cdot \mathbf{k})^2/\rho_0] \sin \beta. \tag{58}$$

The calculated recovery/bleach ratios would accordingly be changed. The accuracy of

replacing Eq. 58 by Eq. 3 can readily be checked for any particular case. For example, using the linear approximation Eq. 3 one can show that for a spherical vesicle, and ($\|$, $\|$, $\epsilon = 0$), the calculated fractional bleach (I_2/I_1) is $5\lambda\mu^2/7\rho_0$. Thus, if the observed fraction bleached is 0.10, then the linear term in the expansion of Eq. 58 is no larger than 0.14, and the quadratic term is no larger than $(1/2!)(0.14)^2$. Thus the quadratic and higher terms can usually be dropped for a bleach of the order of 10%.

Our measured recovery times, σ, do not depend significantly on the fractional bleach even when the bleach is so large that the observed recovery/bleach ratios R differ significantly from the theoretical values (data not given). We attribute this (fortunate) circumstance to the fact that the expansion of the exponential in Eq. 58 leads ultimately to higher order harmonics ($m > 2$ in Eqs. 6–7), and thus contributions of shorter and shorter decay times to the recovery curves. The short-time recovery amplitudes are evidently too small to detect in our experiments.

It is interesting to note that according to Eq. 58, photobleach curves (for bleaches much shorter than σ) should not in general be simple exponentials since the angular factor $(\mu \cdot \mathbf{k}')^2$ appears in the exponential. Only in the case of nonpolarized radiation and coplanar multibilayers does one expect a simple exponential photobleach curve.

Since the transition dipole of diI lies in the plane of the bilayer membrane ($\epsilon = 0$) our measured exponential recovery time σ is related to the rotation time constant τ in the diffusion equation as follows,

$$\sigma = \tau/4. \tag{59}$$

The data in Fig. 6 give recovery times σ for diI in coplanar multibilayer membranes as well as liposomes containing DSPC and various mole fractions of cholesterol, up to 20 mol %. Data are also given for coplanar multibilayer membranes containing DPPC and cholesterol. There is extensive evidence that in binary mixtures of cholesterol and a phosphatidylcholine, at a temperature below the chain melting temperature of the phosphatidylcholine, two phases are present. One is essentially pure "solid" crystalline phosphatidylcholine and a the other is a fluid mixture containing 20 mol % cholesterol (provided the overall cholesterol concentration is <20 mol %) (Owicki and McConnell, 1980; Copeland and McConnell, 1980; Recktenwald and McConnell, in press). The amount of fluid (solid) phase increases (decreases) linearly with increasing mole fraction cholesterol, up to 20 mol %, where the system is entirely fluid.

For binary mixtures of DSPC and cholesterol between 5 and 20 mol % cholesterol, the measured recovery amplitudes I_3–I_2 decrease with increasing concentration (data not shown). No recovery is observed for cholesterol concentrations >20 mol %. This is in accord with the model described above for the cholesterol-phosphatidylcholine mixtures, as rotation of lipid in the fluid phase is too fast to be measured under our present experimental conditions. It is interesting that these very long rotational recovery times (up to 200 s) can be observed since this signifies that these diI molecules do not "visit" the fluid phase during these time periods. The temperature dependence of the rotational recovery time is the same for the various DSPC-cholesterol mixtures, again in accord with this model.

The extension of the present method to the measurement of rotational diffusion times of membrane components in more fluid membranes will require the use of shorter, more intense bleach bursts. It is also necessary that membrane components show fluorescence polarization.

APPENDIX

Hopping Rotational Motion

A referee for this paper has correctly pointed out that the assumption of isotropic rotational diffusion (Eq. 5) may not be appropriate for the lipid membranes used in the present work, because at the temperatures used the membranes studied have crystalline order. In other words, a hopping model for the molecular motion may be more appropriate. This alternative model is readily incorporated in the present calculations.

Because of the known packing of hydrocarbon chains in crystalline lipid bilayers (Janiak et al., 1976; Tardieu et al., 1973; Newton et al., 1978) we may assume that the transition dipole moment μ of diI takes up three orientations in the plane of the membrane, γ_1, γ_2 and γ_3, where $|\gamma_1 - \gamma_2| = |\gamma_2 - \gamma_3| = 2\pi/3$. Immediately after the bleach pulse, we then have three populations that can be obtained from Eq. 8 by setting $t = 0$, and $\gamma = \gamma_1$, γ_2 or γ_3: $\rho(\alpha, \beta, \gamma_1, 0) \equiv \rho_1(0)$, $\rho(\alpha, \beta, \gamma_2, 0) \equiv \rho_2(0)$, and $\rho(\alpha, \beta, \gamma_3, 0) \equiv \rho_3(0)$. The kinetic equations governing the change in these populations have the form

$$\begin{aligned} d\rho_1/dt &= -1/T(\rho_1 - \rho_2) - 1/T(\rho_1 - \rho_3) \\ &= -2/T(\rho_1 - \bar{\rho}) + 1/T(\rho_2 - \bar{\rho}) + 1/T(\rho_3 - \bar{\rho}) \end{aligned} \tag{A1}$$

where T^{-1} is the probability per unit time that there is a jump from one specific orientation, say γ_1, to a second specific orientation, say γ_2, and where $\rho_1 \equiv \rho_1(t)$, etc. Since, by definition

$$\bar{\rho} = \tfrac{1}{3}(\rho_1 + \rho_2 + \rho_3) \tag{A2}$$

Eq. (A1) can be rewritten

$$d\rho_1/dt = -3/T(\rho_1 - \bar{\rho}). \tag{A3}$$

Thus, no matter what the initial distribution of population after photobleaching, the population of each orientation approaches its equilibrium value with the same time constant:

$$\begin{aligned} \rho_i(t) &= \bar{\rho} + [\rho_i(0) - \bar{\rho}]e^{-3t/T} \\ i &= 1, 2, 3. \end{aligned} \tag{A4}$$

Thus, Eq. 8 is replaced by three equations, one for each value of γ_1, and each equation has a single exponential factor, $e^{-3t/T}$.

In our multilayers and liposomes it is likely that, no matter what the value of α and β, there is no relation or coherence between the values of γ_1, γ_2, and γ_3 in the different layers. In this case the integration of Eq. 12 is again carried out with only a change of significance: the integration over γ is not over the motion of a single molecule, but is an average over different γ orientations in different layers. It will be seen that all the remaining equations follow as before, the only difference being in the interpretation of the observed decay constant σ. For a hopping rotation between three equivalent orientations,

$$\sigma = T/3 \tag{A5}$$

where T^{-1} is the site-to-site hopping-rate constant.

This paper is dedicated to Norman Davidson on the occasion of his 65th birthday.

We are greatly indebted to Professor John Brauman for the loan of the HP 1774A oscilloscope, Dr. Barton Smith for the loan of the polarization rotator, and Mr. Frank Howard who wrote a number of computer programs used in this work.

This work has been supported by the National Science Foundation grant PCM 77-23586 and by the Alexander Medical Foundation. The laser was borrowed from the San Francisco Laser Center, supported by the National Science Foundation under Grant no. CHE79-16250, awarded to the University of California at Berkeley, in collaboration with Stanford University.

Received for publication 1 March 1981 and in revised form 8 June 1981.

REFERENCES

Austin, R. H., S. S. Chan, and T. M. Jovin. 1979. Rotational diffusion of cell surface components by time-resolved phosphorescence anisotropy. *Proc. Natl. Acad. Sci. U. S. A.* 76:5650–5654.

Axelrod, D. 1979. Carbocyanine dye orientation in red cell membrane studied by microscopic fluorescence polarization. *Biophys. J.* 26:557–574.

Brown, P. K. 1972. Rhodopsin rotates in the visual receptor membrane. *Nature New Biol.* 236:35–38.

Cherry, R. J. 1978. Measurement of protein rotational diffusion in membranes by flash photolysis. *Methods Enzymol.* 54:47–61.

Cherry, R. J. 1979. Rotational and lateral diffusion of membrane proteins. *Biochim. Biophys. Acta.* 559:289–327.

Cone, R. A. 1972. Rotational diffusion of rhodopsin in the visual receptor membrane. *Nature New Biol.* 236:39–43.

Copeland, B. R., and H. M. McConnell. 1980. The rippled structure in bilayer membranes of phosphatidylcholine and binary mixtures of phosphatidylcholine and cholesterol. *Biochim. Biophys. Acta.* 599:95–109.

Eldridge, C. A., E. L. Elson, and W. W. Webb. 1980. Fluorescence photobleaching recovery methods of surface lateral mobilities on normal and SV40-transformed mouse fibroblasts. *Biochemistry.* 19:2075–2079.

Gaffney, B. J. 1979. Spin label-thiourea adducts. A model for saturation transfer EPR studies of slow anisotropic rotation. *J. Phys. Chem.* 83:3345–3349.

Hyde, J. S., and L. R. Dalton. 1979. Saturation-transfer spectroscopy. *In* Spin Labeling. Vol. II. L. Berliner, editor. Academic Press, Inc., N.Y. 3–70.

Janiak, M. J., D. M. Small, and G. G. Shipley. 1976. Nature of the thermal pretransition of synthetic phospholipids: dimyristoyl- and dipalmitoyllecithin. *Biochemistry.* 15:4575–4580.

Lo, M. M. S., P. B. Garland, J. Lamprecht, and E. A. Barnard. 1980. Rotational mobility of the membrane-bound acetylcholine receptor of *Torpedo* electric organ measured by phosphorescence depolarisation. *FEBS (Fed. Eur. Biochem. Soc.) Lett.* 111:407–412.

Newton, C., W. Pangborn, S. Nir, and D. Papahadjopolous. 1978. Specificity of Ca^{2+} and Mg^{2+} binding to phosphatidylserine vesicles and resultant phase changes of bilayer membrane structure. *Biochim. Biophys. Acta.* 506:281–287.

Nigg, E. A., and R. J. Cherry. 1979. Influence of temperature and cholesterol on the rotational diffusion of band 3 in the human erythrocyte membrane. *Biochemistry.* 18:3459–3465.

Owicki, J. C., and H. M. McConnell. 1980. Lateral diffusion in inhomogeneous membranes. Model membranes containing cholesterol. *Biophys. J.* 30:383–397.

Recktenwald, D. J., and H. M. McConnell. 1981. Phase equilibria in binary mixtures of phosphatidylcholine and cholesterol. *Biochemistry.* 20:4505–4510.

Rousselet, A., J. Cartaud, and P. F. Devaux. 1979. Importance des interactions proteine-proteine dans le maintien de la structure des fragments excitables de l'organe electrique de *Torpedo marmorata*. *Compt. Rend.* 289:461–463.

Rubenstein, J. L. R., B. A. Smith, and H. M. McConnell. 1979. Lateral diffusion in binary mixtures of cholesterol and phosphatidylcholines. *Proc. Natl. Acad. Sci. U. S. A.* 76:15–18.

Schlessinger, J., Y. Schechter, P. Cuatrecasas, M. C. Willingham, and I. Pastan. 1978. Quantitative determination of the lateral diffusion coefficients of the hormone-receptor complexes of insulin and epidermal growth factor on the plasma membrane of culture fibroblasts. *Proc. Natl. Acad. Sci. U. S. A.* 75:5353–5357.

Sheetz, M. P., M. Schindler, and D. E. Koppell. 1980. Lateral mobility of integral membrane proteins is increased in spherocytic erythrocytes. *Nature (Lond.).* 285:510–512.

Shimshick, E. J., and H. M. McConnell. 1973. Lateral phase separations in phospholipid membranes. *Biochemistry.* 12:2351–2360.

Smith, B. A., and H. M. McConnell. 1978. Determination of molecular motion in membranes using periodic pattern photobleaching. *Proc. Natl. Acad. Sci. U. S. A.* 75:2759–2763.

Smith, L. M., J. W. Parce, B. A. Smith, and H. M. McConnell. 1979. Antibodies bound to lipid haptens in model membranes diffuse as rapidly as the lipids themselves. *Proc. Natl. Acad. Sci. U. S. A.* 76:4177–4179.

Tardieu, A., and V. Luzzati. 1976. Structure and polymorphism of the hydrocarbon chains of lipids: a study of lecithin-water phases. *J. Mol. Biol.* 75:711–733.

Thomas, D. D. 1978. Large-scale rotational motions of proteins detected by electron paramagnetic resonance and fluorescence. *Biophys. J.* 24:439–462.

Vaz, W. L. C., R. H. Austin, and H. Vogel. 1979. The rotational diffusion of cytochrome b_5 in lipid bilayer membranes. Influence of the lipid physical state. *Biophys. J.* 26:415–426.

Weber, G. 1973. Fluorescence Techniques in Cell Biology. A. A. Thaer and M. Serndy, editors. Springer-Verlag, Berlin. 5.

Yguerabide, J. and L. Stryer. 1971. Fluorescence spectroscopy of an oriented model membrane. *Proc. Natl. Acad. Sci. U. S. A.* 68:1217–1221.